Mon. Not. R. Astron. Soc. **000**, 1–6 (2004) Printed 2 February 2008 (MN LaTeX style file v2.2)

arXiv:astro-ph/0407187v1 9 Jul 2004

Does regenerated emission change the high-energy signal from gamma-ray burst afterglows?

Shin'ichiro Ando*
Department of Physics, School of Science, The University of Tokyo, 7-3-1 Hongo, Bunkyo-ku, Tokyo 113-0033, Japan

Submitted 9 June 2004; accepted 8 July 2004

ABSTRACT
We study regenerated high-energy emission from the gamma-ray burst (GRB) afterglows, and compare its flux with the direct component from the same afterglow. When the intrinsic emission spectrum extends to TeV region, these very high-energy photons are significantly absorbed by the cosmic infrared background (CIB) radiation field, creating electron/positron pairs; since these pairs are highly energetic, they can scatter the cosmic microwave background radiation up to GeV energies, which may change the intrinsic afterglow light curve in the GeV region. Using the theoretical modeling given in literature and the reasonable choice of relevant parameters, we calculate the expected light curve due to the regeneration mechanism. As the result, we find that the regenerated emission could only slightly change the original light curve, even if we take a rather large value for the CIB density, independently of the density profile of surrounding medium, i.e., constant or wind-like profile. This ensures us the reliable estimation of the intrinsic GRB parameters when the high-energy observation is accessible, regardless of a large amount of uncertainty concerning the CIB density as well as extragalactic magnetic field strength.

Key words: gamma-rays: bursts – diffuse radiation – magnetic fields.

1 INTRODUCTION

Gamma-ray bursts (GRBs) are known to be highly energetic astrophysical objects located at cosmological distance. Accumulated data of many GRBs strongly support relativistic fireball scenario, in which γ-rays up to MeV are attributed to internal shocks due to collisions between fireball shells, while their transient component, afterglow, from radio to X-rays is attributed to external shocks due to the interaction of the fireball with external medium. In addition to such signals, very high-energy photons that range from a few tens of MeV to GeV have been detected (Hurley et al. 1994), and further the detection of an excess of TeV photons from GRB 970417a has been claimed with a chance probability $\sim 1.5 \times 10^{-3}$ (Atkins et al. 2000). Although the statistics of these high-energy signals are not sufficient yet, planned future satellites or detectors will promisingly enable us to discuss high-energy emission mechanisms of GRBs.

Several emission mechanisms of GeV–TeV photons are proposed, such as synchrotron self-inverse Compton (IC) emission of the electrons (Mészáros, Rees & Papathanassiou 1994; Waxman 1997; Panaitescu & Mészáros 1998; Wei & Lu 1998, 2000; Dermer, Böttcher & Chiang 2000a; Dermer, Chiang & Mitman 2000b; Panaitescu & Kumar 2000; Sari & Esin 2001; Zhang & Mészáros 2001) and the proton-synchrotron emission (Vietri 1997; Böttcher & Dermer 1998; Totani 1998), as well as some other hadron-related emission components (Böttcher & Dermer 1998). These mechanisms could be valid for internal shocks, external forward shocks, or external reverse shocks of GRBs.

Regardless of the emission mechanism, high-energy photons above ~ 100 GeV are expected to be attenuated via the $\gamma\gamma \to e^+e^-$ process. Target photons with which the initial high-energy photons interact are the GRB emission itself or the cosmic infrared background (CIB). As for the latter, it is suggested that such very high-energy photons may largely be absorbed during its propagation, if the GRB location is sufficiently cosmological as $z \gtrsim 1$ (Stecker, de Jager & Salamon 1992; MacMinn & Primack 1996; Madau & Phinney 1996; Malkan & Stecker 1998; Salamon & Stecker 1998). Therefore, the detection of TeV photons from cosmological GRBs will be very difficult. However, since created electron/positron pairs due to the interaction with CIB photons are very energetic, they can IC scatter on the most numerous cosmic microwave background (CMB) photons, giving rise to a delayed secondary MeV–GeV emission (Plaga 1995; Cheng & Cheng 1996; Dai & Lu 2002; Wang et al. 2004; Razzaque, Mészáros & Zhang 2004). These regenerated emissions would, therefore, be indirect evidence of

---

* E-mail: ando@utap.phys.s.u-tokyo.ac.jp

the intrinsic TeV emission as well as a probe of the CIB radiation field, which is not satisfactorily constrained. It has been argued that the internal shocks (Dai & Lu 2002; Razzaque et al. 2004) as well as the prompt phase of the external shocks (Wang et al. 2004) are possibly responsible for these delayed MeV–GeV emission, and it would be distinguishable from a different delayed GeV component due to the direct IC emission from the afterglow.

Future detection of the direct MeV–GeV emission predicted from the afterglow, would be a probe of an emission mechanism of the high-energy region as well as physical parameters of the fireball. However, the primary emission is possibly modified when we consider the regenerated light due to an absorption of TeV photons by CIB, and estimating its flux is a nontrivial problem; if the regenerated light significantly changes the high-energy emission profile, it gives a quite large amount of uncertainty on the GRB physics since the CIB background as well as extragalactic magnetic field strength, both of which are not satisfactorily constrained yet, alters the expected signal. In this paper, therefore, we investigate the effects of the delayed emission on the primary afterglow light curve in the GeV range; as a source of the regenerated GeV emission, we consider an afterglow phase itself, which is well described by an external shock model, while the other phases have already been investigated in several papers (Dai & Lu 2002; Wang et al. 2004; Razzaque et al. 2004). Among several mechanisms that predict an afterglow spectrum extending to TeV range, we adopt the IC scattering of the synchrotron photons and follow the formulation given by Zhang & Mészáros (2001) and Sari & Esin (2001); this is because the high-energy emission up to TeV region is most likely realized due to the IC mechanism (Zhang & Mészáros 2001), and the required values for relevant parameters appear to be realized in many GRBs (Panaitescu & Kumar 2002). We show that the regenerated GeV emission, due to the TeV absorption and following CMB scattering, can only slightly changes the detected signals. Therefore, we conclude that the GeV light curves obtained by the future detectors such as the *Gamma-Ray Large Area Space Telescope (GLAST)* surely give us intrinsic information concerning the GRB fireball, not affected by the uncertainty of the CIB as well as the extragalactic magnetic fields.

This paper is organized as follows. In § 2, we briefly summarize the formulation of the prompt high-energy emission given in literature, and then in § 3, we describe the regeneration mechanism from the prompt high-energy emission and give formulation for that. The result of the numerical calculation using a reasonable parameter set is presented in § 4, and finally, we discuss that result and give conclusions in § 5.

2 HIGH-ENERGY RADIATION FROM AFTERGLOWS

As for evolution of the fireball and radiation spectrum, we follow the formulation given in Zhang & Mészáros (2001) and Sari & Esin (2001), and refer the reader to the literature for a detailed discussion; here we briefly summarize necessary information.

The spectrum of the afterglow synchrotron emission (Sari, Piran & Narayan 1998) has breaks at several frequencies, i.e., the self-absorption frequency ν_a, injection frequency ν_m corresponding to the minimum electron Lorentz factor γ_m, cooling frequency ν_c corresponding to the electron Lorentz factor γ_c for which the radiative timescale equals the dynamical time, and cutoff frequency ν_u corresponding to γ_u above which electrons cannot be accelerated. Break frequencies relevant for this study and peak flux are given by

$$\begin{aligned}
\nu_m &= 2.9 \times 10^{16}\,\mathrm{Hz}\ \epsilon_e^2 \epsilon_B^{1/2} \mathcal{E}_{52}^{1/2} t_h^{-3/2} (1+z)^{1/2}, && (1)\\
\nu_c &= 3.1 \times 10^{13}\,\mathrm{Hz}\ (1+Y_e)^{-2} \epsilon_B^{-3/2} \mathcal{E}_{52}^{-1/2} n^{-1} \\
&\quad \times t_h^{-1/2} (1+z)^{-1/2}, && (2)\\
\nu_u &= 2.3 \times 10^{22}\,\mathrm{Hz}\ (1+Y_e)^{-1} \mathcal{E}_{52}^{1/8} n^{-1/8} t_h^{-3/8} \\
&\quad \times (1+z)^{-5/8}, && (3)\\
F_{\nu,\mathrm{max}} &= 29\,\mathrm{mJy}\ \epsilon_B^{1/2} \mathcal{E}_{52} n^{1/2} D_{L,28}^{-2} (1+z), && (4)
\end{aligned}$$

where z is the redshift of the GRB, $\mathcal{E}_{52}$ is the fireball energy per unit solid angle in units of 10^{52} ergs sr^{-1}, n the external medium density in units of cm^{-3}, ϵ_e and ϵ_B represent the fraction of the kinetic energy going to the electrons and magnetic fields, respectively, t_h is the observer time measured in hours, and $D_{L,28}$ is the burst luminosity distance measured in units of 10^{28} cm. The Compton parameter Y_e is given as a ratio between the luminosities due to IC and synchrotron radiation, and can be represented by $Y_e = L_{\mathrm{IC}}/L_{\mathrm{syn}} = [-1 + (1 + 4\eta\epsilon_e/\epsilon_B)^{1/2}]/2$, where $\eta = \min[1, (\gamma_m/\gamma_c)^{p-2}]$ with p representing the spectral index of injected electrons (Panaitescu & Kumar 2000; Sari & Esin 2001).

The IC spectrum due to the scattering on the synchrotron seed photons can be very hard if the Compton parameter Y_e is sufficiently large. The typical break frequencies that characterize the IC spectrum are $\nu_m^{\mathrm{IC}} \simeq \gamma_m^2 \nu_m$ and $\nu_c^{\mathrm{IC}} \simeq \gamma_c^2 \nu_c$. The cutoff frequency in the IC component is defined by $\nu_u^{\mathrm{IC}} = \min(\gamma_u^2 \nu_u, \nu_{\mathrm{KN}}^{\mathrm{IC}})$, where $\nu_{\mathrm{KN}}^{\mathrm{IC}}$ is the Klein-Nishina limit, above which the IC cross section is suppressed. Sari & Esin (2001) explicitly gave analytic expressions for the IC spectrum, and they pointed out that the power-law approximation is no longer accurate at high-frequency region, on which we focus in this paper. Therefore, we use their analytic expressions shown in Appendix A of Sari & Esin (2001), on the contrary to Zhang & Mészáros (2001), in which the authors used an power-law expression for simplicity. High-energy photons reaching to TeV due to the IC scatterings are absorbed by the soft photons in the fireball and create the electron/positron pairs. We follow the treatment of Zhang & Mészáros (2001) for this intrinsic absorption (see also, Lithwick & Sari 2001; Coppi & Blandford 1990; Böttcher & Schlickeiser 1997; Dermer et al. 2000b).

Until this point, we described the emission property in the case that the density profile of surrounding matter is uniform, i.e., n does not depend on the radius. We also consider the case of the wind density profile, which is possibly the case because the GRB progenitors can eject envelope as a stellar wind; assuming a constant speed of the wind, the density profile becomes $n(r) = Ar^{-2}$, where A is a constant independent of radius r. We normalize this constant A as $A = 3.0 \times 10^{35} A_* \ \mathrm{cm}^{-1}$ where $A_* = (\dot{M}/10^{-5} M_\odot \ \mathrm{yr}^{-1})/(v/10^3 \ \mathrm{km\ s}^{-1})$ as in Chevalier & Li (2000) for a Wolf-Rayet star. The relevant frequencies and the peak flux are then be represented by

$$\begin{aligned}
\nu_m &= 2.8\times10^{16}\ \mathrm{Hz}\ \epsilon_e^2\epsilon_B^{1/2}\mathcal{E}_{52}^{1/2}t_h^{-3/2}(1+z)^{1/2}, & (5)\\
\nu_c &= 2.4\times10^{11}\ \mathrm{Hz}\ (1+Y_e)^{-2}\epsilon_B^{-3/2}\mathcal{E}_{52}^{1/2}A_*^{-2}\\
&\quad\times t_h^{1/2}(1+z)^{-3/2}, & (6)\\
\nu_u &= 1.3\times10^{22}\ \mathrm{Hz}\ (1+Y_e)^{-1}\mathcal{E}_{52}^{1/4}A_*^{-1/4}t_h^{-1/4}\\
&\quad\times(1+z)^{-3/4}, & (7)\\
F_{\nu,\max} &= 0.33\ \mathrm{Jy}\ \epsilon_B^{1/2}\mathcal{E}_{52}^{1/2}A_*t_h^{-1/2}D_{L,28}^{-2}(1+z)^{3/2}, & (8)
\end{aligned}$$

following the discussion given in Zhang & Mészáros (2001), which is applied to the case of wind profile. Both the synchrotron and IC spectra at some fixed time are obtained by using the same procedure already given above, but the time evolution of these spectra changes since the dynamics of an expanding jet differs from the case of constant medium. Although we do not give full representation of the spectral evolution, the reader is referred to Panaitescu & Kumar (2000) for analytic treatment including the wind-like structure.

3 INTERACTION WITH COSMIC INFRARED BACKGROUND AND REGENERATED HIGH-ENERGY EMISSION

For typical GRB locations at redshift $z = 1$, Salamon & Stecker (1998) indicated that the optical depth due to the CIB radiation field reaches ~ 10 when the energy of *prompt* emission is higher than 300 GeV. We assume that the electron and positron of the $e^{\pm}$ pair share 1/2 the photon energy, i.e., $\gamma_e = \epsilon_\gamma/2m_e$. With this assumption, the created electron/positron spectrum can be described by

$$\frac{d^2N_e}{dt_p d\gamma_e} = 2\frac{d\nu}{d\gamma_e}\frac{F_\nu(t_p,\epsilon_\gamma)}{\epsilon_\gamma} = \frac{2}{h\gamma_e}F_\nu(t_p, 2m_e\gamma_e), \tag{9}$$

where $\epsilon_\gamma = h\nu$, t_p represents the observed time of the prompt emission provided that there is no absorption by the CIB, and F_ν is the flux of prompt photons including the intrinsic absorption. Following the result of Salamon & Stecker (1998), we assume that the high-energy photons with $\epsilon_\gamma > 300$ GeV are completely attenuated, creating $e^{\pm}$ pairs with $\gamma_e > 3\times10^5$. The pair creations typically occur at the distance $R_{\rm pair} = (0.26\sigma_T n_{\rm IR})^{-1} \simeq 5.8\times10^{24}\,{\rm cm}^{-3}(n_{\rm IR}/1\,{\rm cm}^{-3})^{-1}$, where $n_{\rm IR}$ is the CIB number density; this length scale is much less than the distance from the observer to the GRB, D_L, and hence, the attenuation of the primary photons can be regarded as quite local phenomenon.

The secondary electron/positron pairs then IC scatter the CMB photons up to GeV energy scale, and pairs cool on a timescale $t_{\rm IC} = 3m_ec/(4\gamma_e\sigma_T u_{\rm cmb}(z)) \approx 7.3\times10^{13}(\gamma_e/10^6)^{-1}(1+z)^{-4}$ s in the local rest frame, where $u_{\rm cmb}(z)$ represents the CMB energy density at redshift z. The IC spectrum from an electron (positron) with the Lorentz factor γ_e, scattering on a CMB photon whose energy is $\epsilon_{\rm cmb}$, $d^3N_\gamma/d\epsilon_{\rm cmb}dt'_d dE_\gamma$, is explicitly given by Blumenthal & Gould (1970) to be

$$\begin{aligned}
\frac{d^3N_\gamma}{d\epsilon_{\rm cmb}dt'_d dE_\gamma} &= \frac{\pi r_0^2 c}{2\gamma_e^2}\frac{n_{\rm cmb}(\epsilon_{\rm cmb},z)}{\epsilon_{\rm cmb}^2}\left(2E_\gamma\ln\frac{E_\gamma}{4\gamma_e^2\epsilon_{\rm cmb}}\right.\\
&\qquad\left.+E_\gamma + 4\gamma_e^2\epsilon_{\rm cmb} - \frac{E_\gamma^2}{2\gamma_e^2\epsilon_{\rm cmb}}\right), \qquad (10)
\end{aligned}$$

where $n_{\rm cmb}(\epsilon_{\rm cmb}, z)$ is the number spectrum of the CMB at redshift z, t'_d represents the time of the delayed emission in the local rest frame, measured from the onset of the $e^{\pm}$ pair generation, and E_γ the energy of the delayed γ-ray. Since the observed time of the delayed emission t can be represented by $t = t_p + t_d$, where t_d is the observed time of the delayed emission measured from the pair generation, the flux of the regenerated γ-ray is obtained by

$$F_\nu(t, E_\gamma) = \int_0^t dt_p\ E_\gamma\ \left.\frac{d^3N_{\rm delayed\ IC}}{dt_p dt_d dE_\gamma}\right|_{t_d=t-t_p}, \tag{11}$$

where

$$\begin{aligned}
\frac{d^3N_{\rm delayed\ IC}}{dt_p dt_d dE_\gamma} &= \int d\epsilon_{\rm cmb}\int d\gamma_e\left(\frac{d^2N_e}{dt_p d\gamma_e}\right)\\
&\quad\times\left(\frac{d^3N_\gamma}{d\epsilon_{\rm cmb}dt'_d dE_\gamma}\right)t_{\rm IC}(\gamma_e)\frac{e^{-t_d/\Delta t(\gamma_e)}}{\Delta t(\gamma_e)}, \qquad (12)
\end{aligned}$$

which can be calculated with the previously evaluated spectra (eqs. [9] and [10]). Here, the lower bound of the integration over γ_e is $\max[3\times10^5, (E_\gamma/\epsilon_{\rm cmb})^{1/2}/2]$. In equation (12), $(d^3N_\gamma/d\epsilon_{\rm cmb}dt'_d dE_\gamma)t_{\rm IC}$ shows a total number of the IC photons per unit CMB energy per unit IC photon energy, emitted until the parent electron with γ_e cools. The last part of the same equation $e^{-t_d/\Delta t}/\Delta t$ represents the time profile of the delayed γ-ray emission, and $\Delta t(\gamma_e)$ is the typical observed duration of the IC photons from the electron (positron) with Lorentz factor γ_e. The typical timescale of the delayed emission measured in the observer frame is given by $\Delta t(\gamma_e) = \max(\Delta t_{\rm IC}, \Delta t_A, \Delta t_B)$, where $\Delta t_{\rm IC} = (1+z)t_{\rm IC}/2\gamma_e^2$ is the IC cooling time; $\Delta t_A = (1+z)R_{\rm pair}/2\gamma_e^2 c$ is the angular spreading time; and $\Delta t_B = (1+z)t_{\rm IC}\theta_B^2/2$ is the delay time due to magnetic deflection. The deflection angle θ_B is given by $\theta_B \approx 1.3\times10^{-5}(\gamma_e/10^6)^{-2}B_{{\rm IG},-20}$, where $B_{{\rm IG},-20}$ represents the extragalactic magnetic field strength in units of 10^{-20} G.

4 RESULTS

We calculated the expected high-energy signal in the GeV range due to the prompt and regenerated afterglow emissions using equation (11) as well as the formulation given by Zhang & Mészáros (2001) and Sari & Esin (2001). In the following discussion, we fix several relevant parameters used in our calculation as follows: $\mathcal{E}_{52} = 10, n = 1, A_* = 1, z = 1$, and $B_{{\rm IG},-20} = 1$.

As for the parameters ϵ_e and ϵ_B, we first fix them at 0.5 and 0.01, respectively. Figure 1(a) shows a fluence $\int_{\nu_1}^{\nu_2}F_\nu d\nu\ t$ as a function of observed time t, where $h\nu_1 = 400$ MeV and $h\nu_2 = 200$ GeV; the lower three curves represent the fluence of the regenerated emission in the case of $n_{\rm IR} = 1$ (dashed curve), 0.1 (solid curve), and 0.01 cm^{-3} (dot-dashed curve). Total fluence from the prompt and delayed afterglow components are shown as upper three (almost degenerate) curves using the same line type according to the CIB density. The fluence threshold for the *GLAST* satellite is roughly $\sim 4\times10^{-7}(t/10^5\ {\rm s})^{1/2}$ ergs cm^{-2} for a long integration time regime (exposure time $t \gtrsim 10^5$ s) and $\sim 4\times10^{-7}$ ergs cm^{-2} for a short integration time, following the criterion that at least 5 photons are collected (Gehrels & Michelson

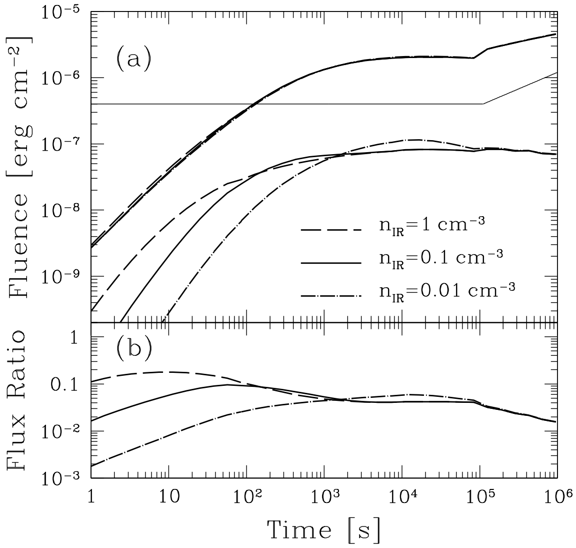

Figure 1. (a) Fluence $\int_{\nu_1}^{\nu_2} F_\nu d\nu \, t$ as a function of observed time t, integrated over 400 MeV to 200 GeV. Lower three curves show the fluence of the regenerated emission in the case of $n_{\rm IR} = 1$ (dashed curve), 0.1 (solid curve), and 0.01 cm^{-3} (dot-dashed curve). Upper three (almost degenerate) curves show the total fluence. The values for the relevant parameters are: $\mathcal{E}_{52} = 10, n = 1, \epsilon_e = 0.5, \epsilon_B = 0.01, z = 1$, and $B_{{\rm IG},-20} = 1$. The sensitivity curve of the *GLAST* satellite is also shown. (b) Flux ratio of the delayed and prompt afterglow emission, integrated over the same energy range.

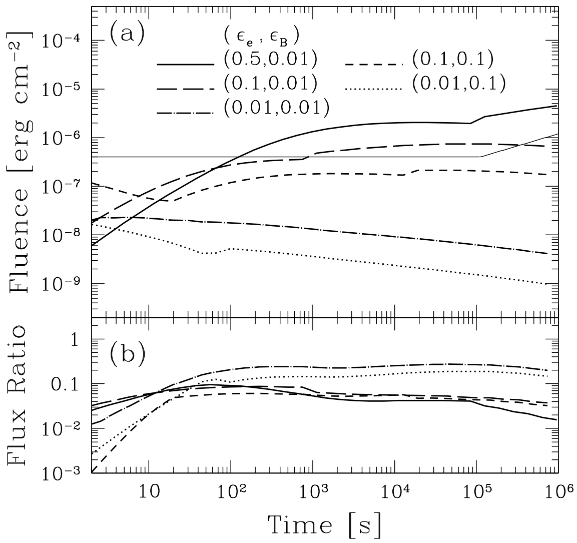

Figure 2. The same as figure 1, but for various sets of (ϵ_e, ϵ_B) with fixed value of $n_{\rm IR} = 0.1$ cm^{-3}. Total fluence alone is shown in the upper panel (a).

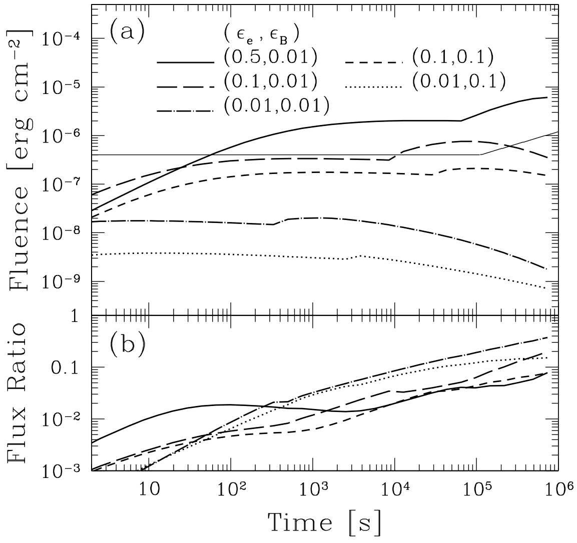

Figure 3. The same as figure 2, but for the wind-like profile of surrounding medium with $A_* = 1$.

1999; Zhang & Mészáros 2001); this sensitivity curve is also plotted in the same figure as a thin solid line.

Figure 1(b) shows a ratio of the regenerated and prompt flux integrated over the same energy range. From these figures, it is found that the contribution from the regenerated GeV emission due to the absorption by the CIB photons peaks around 10–10^4 s after the onset of the afterglow, according to the CIB density. This is because the time delay occurs mainly by the angular spreading at the location of the absorption, $\Delta t_A \propto n_{\rm IR}^{-1}$. The regenerated emission is expected to only slightly change the afterglow light curve even when we adopt a rather large value of $n_{\rm IR}$; for $n_{\rm IR} = 1$ cm^{-3}, its contribution reaches $\sim 20\%$ of the prompt emission around 10 s, but the total fluence around that time is far below the detection threshold.

By fixing $n_{\rm IR}$ to be 0.1 cm^{-3}, we then investigated the dependence of the GeV light-curve on ϵ_e and ϵ_B; the result is shown in figure 2. Curves in figure 2(a) indicate the total fluence evaluated using various sets of (ϵ_e, ϵ_B), and the ratio of regenerated and prompt emission is shown in figure 2(b). As we expect, rather large values of ϵ_e are favourable for possible detection by the *GLAST*, because they make the spectrum extend to high-energy region owing to the IC scattering. In the case of the small ϵ_e, on the other hand, the flux in the GeV region is not as strong as the case of large ϵ_e, as already discussed in several past papers (e.g., Zhang & Mészáros 2001). Regardless of the detectability of the total emission, it is easily found that the regenerated emission is very weak compared with the prompt one, at most $\sim 30\%$ if the value of ϵ_B is large, as shown in figure 2(b).

The result of the same calculation is shown for the case of wind-like profile of surrounding matter, $n(r) \propto r^{-2}$, in figure 3 for various values of (ϵ_e, ϵ_B); other parameters are the same as figure 2 except for $A_* = 1$. We can confirm that the GeV light-curves as well as their parameter dependence are basically similar to the case of constant density profile. The fraction of the regenerated flux to the prompt one shown in figure 3, on the other hand, behaves somewhat differently;

it increases as the time pasts. However, it reaches only less than 40% at 10^6 s after the onset of the afterglow, after which the detection threshold for the fluence glows as $t^{1/2}$ and the detection itself becomes more and more difficult. Furthermore, favourable model with large ϵ_e gives smaller contribution from the regenerated emission than the models with small ϵ_e, which is not favoured from the viewpoint of detectability. In consequence, the regenerated emission gives only very slight correction to the prompt afterglow emission in the GeV region, and further, it is found that this characteristic is considerably independent of the relevant parameters such as $n_{\rm IR}$, ϵ_e, and ϵ_B as well as the density profile of the surrounding medium.

5 DISCUSSION AND CONCLUSIONS

In recent years, it is suggested that the delayed GeV emission, due to the absorption of the TeV photons by the CIB radiation field and the following IC scattering on the CMB photons, may be detected by the future high-energy detectors such as the *GLAST*. As a source of the original TeV emissions, the internal shocks (Dai & Lu 2002; Razzaque et al. 2004) as well as the initial phase of the external shocks (Wang et al. 2004) have been considered. These authors claim that the delayed emission due to the regeneration process during propagation can be distinguished from the direct GeV component due to the IC emission in the afterglow phase.

The emission from the afterglows is also expected to extend to TeV region with reasonable choices of relevant parameters, and then the afterglow phase itself can also be a source of the regenerated emission. Since an estimation of this regenerated emission has not been performed yet, and further, whether its intensity is above the detection threshold is nontrivial question, we investigated in this paper the evolution of the regenerated light from the afterglows, and discussed its detectability. As an original high-energy emission model that extends to TeV region, we have used the modeling of the synchrotron self-IC mechanism by Zhang & Mészáros (2001) and Sari & Esin (2001), and also used reasonable choices of relevant parameters.

As the result of calculation using formalism summarized in § 3 and the constant density profile as well as $\epsilon_e = 0.5$ and $\epsilon_B = 0.01$, we found that the contribution of the regeneration of GeV photons could give a correction at most $\sim 20\%$ even if rather large value for the CIB density ($n_{\rm IR} = 1$ cm^{-3}) is used as shown in figure 1. Although the CIB density around $z = 1$ is unknown, observations suggest that the local CIB flux at 2.2 μm is of the order of 10 nW m^{-2} sr^{-1} (Wright & Johnson Wright & Johnson; Wright 2004), which corresponds to $n_{\rm IR} = 0.45 \times 10^{-2}$ cm^{-3}. Theoretical model by Salamon & Stecker (1998) indicates that the comoving density of the CIB photons does not change largely (i.e., less than factor of ~ 3) from $z = 1$ to 0, and therefore the proper density of the CIB might be estimated to be around 0.1 cm^{-3}, although there remains a fair amount of ambiguity. Our calculation suggests that even if we take a fairly large value for the CIB density, the regenerated emission cannot change the shape of the intrinsic light curve, and further, its intensity is far below the detection threshold of the *GLAST* satellite.

In addition to the cosmic CIB density, extragalactic magnetic field strength may affect the results of our calculation via the value of Δt_B appearing in equation (12) if it is larger than 10^{-20} G that we used throughout the above discussions. The strength of extragalactic magnetic fields has not been determined thus far. Faraday rotation measures imply an upper limit of $\sim 10^{-9}$ G for a field with 1 Mpc correlation length (see Kronberg 1994 for a review). Other methods were proposed to probe fields in the range 10^{-10} to 10^{-21} G (Lee, Olinto & Sigl 1995; Plaga 1995; Guetta & Granot 2003). To interpret the observed microgauss magnetic fields in galaxies and X-ray clusters, the seed fields required in dynamo theories could be as low as 10^{-20} G (Kulsrud et al. 1997; Kulsrud 1999). Theoretical calculations of primordial magnetic fields show that these fields could be of order 10^{-20} G or even as low as 10^{-29} G, generated during the cosmological QCD or electroweak phase transition, respectively (Sigl, Olinto & Jedamzik 1997). Hence, although we used the value of 10^{-20} G as the extragalactic magnetic field strength, it is accompanied by a quite large amount of uncertainty and it may affect the results give above. From figure 1, it is found that when $B_{\rm IG} = 10^{-20}$ G, the time delay of the regenerated emission is mainly dominated by angular spreading, i.e., $\Delta t = \Delta t_A$, because the delayed component changes according to the CIB density $n_{\rm IR}$. For further smaller values of $B_{\rm IG}$ than 10^{-20} G, therefore, our conclusion does not change. On the other hand, if its value is sufficiently large such that the condition $\Delta t_B > \Delta t_A$ is satisfied for the majority of possible γ_e, it further suppresses the regenerated emission since its flux is inversely proportional to Δt_B as clearly shown in equation (12). In consequence, even if the value of extragalactic magnetic fields differs from our reference value, our central conclusion that the regenerated emission is negligibly weak compared with the prompt one does not change.

We also performed the same calculation but by focusing on dependence on the relevant parameters (ϵ_e, ϵ_B) that strongly affect the high-energy emission mechanism. We showed that although the total fluence in the GeV region considerably depends on the values of (ϵ_e, ϵ_B), but the fraction of the regenerated emission to the prompt one is always small for any choices of parameter sets (figure 2). This characteristic holds in the case of the wind-like profile of surrounding medium as shown in figure 3. All of these facts given above enable us to probe a high-energy emission mechanism in the GRB fireballs when data of the GeV photons are accumulated, because the expected signal would be almost completely free of a large amount of uncertainty concerning the CIB density as well as extragalactic magnetic field; they never affect the afterglow emission itself for any choices of the relevant parameters (ϵ_e, ϵ_B), whichever (constant or wind-like) profile of the surrounding medium is truly realized.

ACKNOWLEDGMENTS

This work was supported by a Grant-in-Aid for JSPS Fellows.

REFERENCES

Atkins R., et al., 2000, ApJ, 533, L119

Blumenthal G. R., Gould R. J., 1970, Rev. Mod. Phys., 42, 237

Böttcher M., Dermer C. D., 1998, ApJ, 499, L131

Böttcher M., Schlickeiser R., 1997, A&A, 325, 866

Cheng L. X., Cheng K. S., 1996, ApJ, 459, L79

Chevalier R. A., Li Z. Y., 2000, ApJ, 520, L29

Coppi P. S., Blandford R. D., 1990, MNRAS, 245, 453

Dai Z. G., Lu T., 2002, ApJ, 580, 1013

Dermer C. D., Böttcher M., Chiang J., 2000a, ApJ, 537, 255

Dermer C. D., Chiang J., Mitman K., 2000b, ApJ, 537, 785

Gehrels N., Michelson P., 1999, Astropart. Phys., 11, 277

Guetta D., Granot J., 2003, ApJ, 585, 885

Hurley K., et al., 1994, Nature, 371, 652

Kronberg P. P., 1994, Rep. Prog. Phys., 57, 325

Kulsrud R., 1999, Ann. Rev. A&A, 37, 37

Kulsrud R., Cowley S. C., Gruzinov A. V., Sudan R. N., 1997, Phys. Rep., 283, 213

Lee S., Olinto A. V., Sigl G., 1995, ApJ, 455, L21

Lithwick Y., Sari R., 2001, ApJ, 555, 540

MacMinn D., Primack J. R., 1996, Space Sci. Rev., 75, 413

Madau P., Phinney E. S., 1996, ApJ, 456, 124

Malkan M. A., Stecker F. W., 1998, ApJ, 496, 13

Mészáros P., Rees M. J., Papathanassiou H., 1994, ApJ, 432, 181

Panaitescu A., Kumar P., 2000, ApJ, 543, 66

Panaitescu A., Kumar P., 2002, ApJ, 571, 779

Panaitescu A., Mészáros P., 1998, ApJ, 501, 772

Plaga R., 1995, Nature, 374, 430

Razzaque S., Mészáros P., Zhang B., , 2004, preprint (astro-ph/0404076)

Salamon M. H., Stecker F. W., 1998, ApJ, 493, 547

Sari R., Esin A., 2001, ApJ, 548, 787

Sari R., Piran T., Narayan R., 1998, ApJ, 497, L17

Sigl G., Olinto A. V., Jedamzik K., 1997, Phys. Rev. D, 55, 4582

Stecker F. W., de Jager O. C., Salamon F. W., 1992, ApJ, 390, L49

Totani T., 1998, ApJ, 502, L13

Vietri M., 1997, Phys. Rev. Lett., 78, 4328

Wang X. Y., Cheng K. S., Dai Z. G., Lu T., 2004, ApJ, 604, 306

Waxman E., 1997, ApJ, 485, L5

Wei D. M., Lu T., 1998, ApJ, 505, 252

Wei D. M., Lu T., 2000, A&A, 360, L13

Wright E., 2004, New. Astron. Rev., 48, 465

Wright E., Johnson B., 2001, preprint (astro-ph/0107205)

Zhang B., Mészáros P., 2001, ApJ, 559, 110